CORA Cork Open Research Archive
Cartlann Taighde Oscailte Chorcaí

Title	A first-principle assessment at atomistic scale of interface phenomena in down-scaling hafnium-based metal-insulator-metal diodes
Authors	Laudadio, Emiliano;Aldrigo, Martino;Stipa, Pierluigi;Pierantoni, Luca;Mencarelli, Davide;Dragoman, Mircea;Modreanu, Mircea
Publication date	2023-02-14
Original Citation	Laudadio, E., Aldrigo, M., Stipa, P., Pierantoni, L., Mencarelli, D., Dragoman, M. and Modreanu, M. (2022) 'A first-principle assessment at atomistic scale of interface phenomena in down-scaling hafnium-based metal-insulator-metal diodes', 2022 IEEE MTT-S International Conference on Numerical Electromagnetic and Multiphysics Modeling and Optimization (NEMO), Limoges, France, 6-8 July. doi: 10.1109/NEMO51452.2022.10038975
Type of publication	Conference item
Link to publisher's version	10.1109/NEMO51452.2022.10038975
Rights	© 2022, IEEE. Personal use of this material is permitted. Permission from IEEE must be obtained for all other uses, in any current or future media, including reprinting/republishing this material for advertising or promotional purposes, creating new collective works, for resale or redistribution to servers or lists, or reuse of any copyrighted component of this work in other works.
Download date	2026-11-04 06:01:15
Item downloaded from	https://hdl.handle.net/10468/14309

UCC
University College Cork, Ireland
Coláiste na hOllscoile Corcaigh

A first-principle assessment at atomistic scale of interface phenomena in down-scaling hafnium-based metal-insulator-metal diodes

Emiliano Laudadio[1], Martino Aldrigo[2], Pierluigi Stipa[1], Luca Pierantoni[1], Davide Mencarelli[1], Mircea Dragoman[2], and Mircea Modreanu[3]

[1] Marche Polytechnic University, Via Brecce Bianche, 60131 Ancona, Italy
[2] IMT-Bucharest, 077190 Voluntari (Ilfov), Romania
[3] Tyndall National Institute-University College Cork, Lee Maltings, Dyke Parade, Cork, Ireland

***Abstract* — In this paper, we present first-principle calculations to study the electrical properties of hafnium oxide (HfO_2)-based metal-insulator-metal (MIM) diodes. These devices have been simulated by interposing 3 nm of HfO_2 between drain and source contacts made of gold and platinum, respectively. The monoclinic and orthorhombic polymorphs of HfO_2 have been considered to model different MIM diodes, and the interface geometries have been optimized to compute the *I-V* characteristics. The simulation results demonstrate the influence of the HfO_2 polymorphs on the MIM properties and the importance to understand the interface phenomena that are related to the measurable properties of the proposed devices.**

***Index Terms* — DFT, diodes, ferroelectric materials, hafnium compounds, *I-V* characteristics, interface, optimization.**

I. Introduction

The modelling of interfaces is of utmost importance from the technological point of view since it helps understand better the electrical properties of nanoscale devices. With respect to that, it is mandatory to identify the transitions of bonding characters at metal-oxide interfaces, with dissimilar electronic structures at the two sides, and how they are coupled with the interfacial structural and compositional variations. In this field, the electronic transport properties have been investigated by modelling metal-insulator-metal (MIM) diodes based on hafnium oxide (HfO_2) at atomistic level. The transmission functions have been evaluated by simulating an electric field in two directions, i.e., from the source to the drain and vice-versa. Platinum and gold have been chosen as source and drain, respectively, whereas between the two electrodes a 3-nm-thick HfO_2 layer has been interposed. It is important to stress that gold and platinum can exhibit different Miller indices, thus generating different possible interaction patterns [1-2]. In this paper, two different Miller configurations have been investigated (100 and 110) for both metal types. Another important constraint is placed by HfO_2, which is well known to adopt different polymorphs with different properties [3]. With the aim to investigate the effects of polymorphs on the device properties, monoclinic $P2_1/c$ (m) and orthorhombic $PCa2_1$ (o) phases of HfO_2 have been considered, since the first is the most stable structure and the second has peculiar properties due to its intrinsic ferroelectric behavior [4]. The optimization of the interfaces has been performed using density functional theory (DFT) with the generalized gradient approximation (GGA) exchange-correlation (xc) functional. The semi-local character of this approach leads to neglect the long-range correlation interactions, which capture attractive van der Waals forces. Considering the high number of *d* electrons involved in the chemical bonds on the interfaces, corrective Grimme D3 potentials have been added to DFT: this approach, called DFT-D3 [5], has demonstrated to offer the best tradeoff between high accuracy degree and reasonable simulation time to detect interface phenomena, which can be difficult to observe from experiments. The most stable optimized interfaces have been used to model the proposed MIM diodes and the GGA-PBE approach has been deployed for the calculation of the *I-V* characteristics.

II. Materials and methods

All simulations have been performed using the DFT approach based on the Perdew–Burke–Ernzerhof (PBE) xc functional with norm-conserving Pseudo Dojo pseudopotentials to describe core electrons for each atom type. The optimization of the interfaces has been computed using QuantumEspresso [6]. The single-particle wave functions have been expanded on a basis of plane-wave (PW) functions, and D3 corrective terms have been added using periodic boundary conditions (PBC) along all axes. The calculation of the *I-V* characteristics has been performed using the Quantum Atomistic Toolkit (Q-ATK) software package [7]. For this type of simulations, the single-electron eigenfunctions have been expanded into a set of finite-range atomic-like basis functions following the linear combination of atomic orbital (LCAO) representation. The simulated *I–V* dependences are referred to the specific transversal width of the modelled devices using a combined use of different boundary conditions. In detail, PBC have been used along the x and y axes, whereas a fixed potential has been generated along the z axis using Dirichlet conditions. This approach suggests that a quantitative computationally inexpensive description of coherent transport in solid junctions is readily achievable, enabling new understanding and control of charge transport properties of atomistic-scale interfaces at large bias voltages.

III. Results and Discussions

A. Modelling of interfaces

One of the most important issues is to find the most stable interfaces that maximize the performance of the MIM diode under investigation. With the aim to avoid simulation artifacts, an extensive geometry optimization of the interfaces has been carried out before the calculation of the *I-V* characteristics. Both gold and platinum atomic systems have been considered with Miller indices of 100 and 110 in association with monoclinic HfO_2 (m-HfO_2) and orthorhombic HfO_2 (o-HfO_2). Due to the asymmetry of the orthorhombic unit cell, both lattice orientations have been included. Considering all possible combinations, six HfO_2-Au and six HfO_2-Pt interfaces have been optimized to detect the most stable ones. Analyzing the interfaces with Au (100), stable and relaxed interfaces have been obtained in all cases, whereas the use of Au (110) determined distorted structures with the formation of electronic vacuum regions (Fig. 1). This was evident in the monoclinic form, whereas the asymmetry of the orthorhombic polymorph allows more plausible interfaces although with certain intrinsic stress.

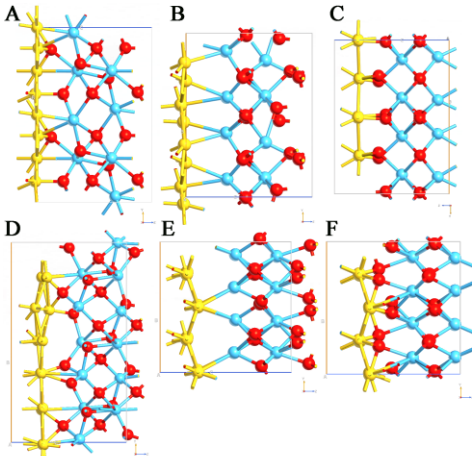


Fig. 1. Optimized Au (100)-*P2₁/c* (a), Au (100)→*Pca2₁* (b), Au (100)←*Pca2₁* (c), Au (110)-*P2₁/c* (d), Au (110)→*Pca2₁* (e), Au (110)←*Pca2₁* (f) interfaces. The arrows indicate the direction of o-polarization. Au, Hf, and O entities are highlighted in yellow, blue, and red, respectively

Regarding the systems with Pt, a similar trend has been observed concerning the Au interfaces, with more evident distortion in all models including Pt (110). An explanation of the larger interface deformation induced by Pt could be related to the stronger bonds formed by this metal with respect to Au (Fig. 2). In fact, gold completely fills the orbitals involved in the chemical bonds with 10 d electrons, whereas platinum has 1 *d* electron less than gold. Both have the same numbers of orbitals, meaning that the lack of one electron to complete the *d* orbitals in Pt leads to stronger chemical bonds [8].

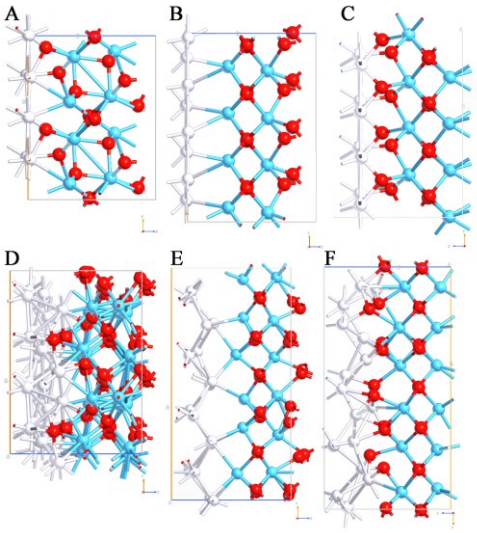


Fig. 2. Optimized Pt (100)-*P2₁/c* (a), Pt (100)→*Pca2₁* (b), Pt (100)←*Pca2₁* (c), Pt (110)-P2₁/c (d), Pt (110)→*Pca2₁* (e), Pt (110)←*Pca2₁* (f) interfaces. The arrows indicate the direction of o-polarization. Pt, Hf, and O entities are highlighted in white, blue, and red, respectively

To verify the intrinsic stress of the interfaces, the cohesive formation energy values have been calculated (Table 1). The adhesion of Pt is about 0.2 eV stronger than that of Au, meaning that Pt is much stronger bonded to the HfO_2 with respect to Au. Moreover, since the o-HfO_2 polymorph may have two opposite orientations, it is worth noticing that the adhesion cohesive energy is -1.54 eV when Pt is directly bonded with O and decreases to 1.12 eV when it is bound to Hf. A similar trend has been found for Au interfaces, underlining the importance of short- and long-range phenomena between different materials.

TABLE 1
ENERGY FORMATIONS OF DIFFERENT INTERFACES

Interface	Cohesive energy
Au(100) - *P2₁/c* HfO_2	-2.64 eV
Au(110) - *P2₁/c* HfO_2	0.75 eV
Au(100) → *Pca2₁* HfO_2	-0.93 eV
Au(110) → *Pca2₁* HfO_2	0.03 eV
Au(100) ← *Pca2₁* HfO_2	-1.31 eV
Au(110) ← *Pca2₁* HfO_2	-0.12 eV
Pt(100) - *P2₁/c* HfO_2	-2.86 eV
Pt(110) - *P2₁/c* HfO_2	0.94 eV
Pt(100) → *Pca2₁* HfO_2	-1.12 eV
Pt(110) → *Pca2₁* HfO_2	0.25 eV
Pt(100) ← *Pca2₁* HfO_2	-1.54 eV
Pt(110) ← *Pca2₁* HfO_2	0.11 eV

B. I-V characteristics

The most stable interfaces based on Au (100) and Pt (100) have been used to model three different MIM diodes. Each of them comprises a 3-nm-thick HfO_2 layer (i.e., one of the studied polymorphs). The dimensions of the final devices are x = 2.44 nm, y = 2.32 nm, and z = 6.68 nm for the m-MIM (Fig. 3A); x = 2.16 nm, y = 2.18 nm, and z = 6.32 nm for the direct o-MIM (Fig. 3B); x = 2.16 nm, y = 2.36 nm, and z = 6.32 nm for the inverse o-MIM (Fig. 3C).

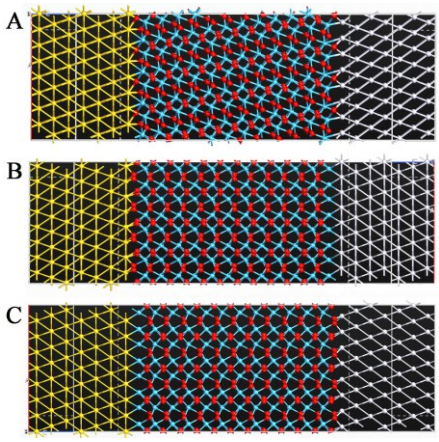


Fig. 3. MIM diodes based on (a) m-HfO_2, (b) o-HfO_2 with polarization directed to drain, and (c) o-HfO_2 with polarization directed to the source

The *I-V* characteristics have been computed and compared, and the results are shown in Fig. 4. While the monoclinic phase diode shows intermediate current values from negative to positive voltages, more evident differences have been observed in the *I-V* characteristics of the two systems containing the orthorhombic phase. Higher current values have been calculated for the system in which the spontaneous polarization of the orthorhombic phase is oriented towards the drain; on the contrary, lower values have been obtained when the o-HfO_2 is oriented towards the source. These results suggest how the exploitation of the ferroelectric phase of HfO_2 could be beneficial for the optimization of the MIM performance for detection and energy-harvesting applications.

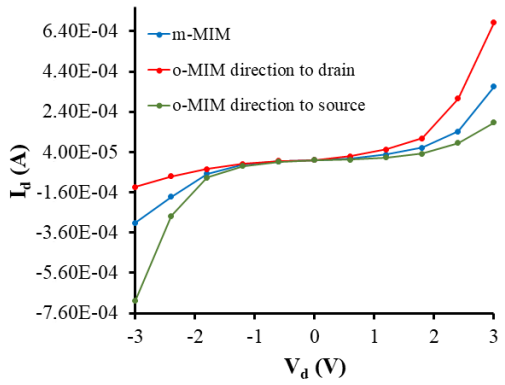


Fig. 4. Calculated *I-V* characteristics of the three modelled MIM diodes

VI. Conclusion

In this work, we have presented the modelling of MIM diodes, including the calculation of their electronic transport properties applying first-principle methods. Our results remark the importance of investigating local phenomena on interfaces and the impact of different components on the measurable properties of the devices.

Acknowledgement

This work was supported in part by the European Project H2020 FETPROACT- EIC-05-2019 "NANO-EH" under Grant 951761, and in part by two grants of the Romanian Ministry of Research, Innovation and Digitalization, CCCDI-UEFISCDI, under Project PN-III-P3-3.6-H2020-2020-0072 and Project PN-III-P2-2.1-PED-2019-0052, within PNCDI III. We would also like to thank the CINECA-HPC ISCRA MARCONI-100 computer system (Project No. HP10CMPMGP).

References

[1] S. Dawei, S. Dou, and G. Wang, "Gold nanocrystals with variable index facets as highly effective cathode catalysts for lithium–oxygen batteries," *NPG Asia Mater,* 7, e155, 2015.

[2] V. P. Santos, and G. A. Camara, "Platinum single crystal electrodes: Prediction of the surface structures of low and high Miller indexes faces," *Results in Surfaces and Interfaces,* 3, 100006, 2021.

[3] E. Laudadio, P. Stipa, L. Pierantoni, and D. Mencarelli, "Phase Properties of Different HfO_2 Polymorphs: A DFT-Based Study," *Crystals,* 12 (1), 90, 2022.

[4] P. Polakowski and J. Müller, "Ferroelectricity in undoped hafnium oxide," *Appl. Phys. Lett.* 106, 232905, 2015.

[5] S. Grimme, J. Antony, S. Ehrlich, and H. Krieg, "A consistent and accurate ab initio parametrization of density functional dispersion correction (DFT-D) for the 94 elements H-Pu," *Chem. Phys.* 132, 154104, 2010.

[6] P. Giannozzi, O. Andreussi, T. Brumme, O. Bunau, M. Buongiorno Nardelli, M. Calandra, *et al.*, "Advanced capabilities for materials modelling with Quantum ESPRESSO," *J. Phys.: Condens. Matter* 29, 465901, 2017.

[7] S. Smidstrup, T. Markussen, P. Vancraeyveld, J. Wellendorff, J. Schneider, T. Gunst, *et al.*, "QuantumATK: An integrated platform of electronic and atomic-scale modelling tools," *J. Phys: Condens. Matter* 32, 015901, 2019.

[8] Q. Cai, X. Wang, and J. Wang, "Distinctions between Supported Au and Pt Catalysts for CO Oxidation: Insights from DFT Study," *J. Phys. Chem. C*, 117, 41, 21331–21336, 2013.